The Bud4 Protein of Yeast, Required for Axial Budding, Is Localized to the Mother/Bud Neck in a Cell Cycle–dependent Manner

Sylvia L. Sanders and Ira Herskowitz

Department of Biochemistry and Biophysics, University of California, San Francisco, California 94143-0448

Abstract. **a** and α cells of the yeast *Saccharomyces cerevisiae* exhibit an axial budding pattern, whereas **a**/α diploid cells exhibit a bipolar pattern. Mutations in *BUD3, BUD4*, and *AXL1* cause **a** and α cells to exhibit the bipolar pattern, indicating that these genes are necessary to specify the axial budding pattern (Chant, J., and I. Herskowitz. 1991. *Cell.* 65:1203–1212; Fujita, A., C. Oka, Y. Arikawa, T. Katagi, A. Tonouchi, S. Kuhara, and Y. Misumi. 1994. *Nature (Lond.).* 372:567–570). We cloned and sequenced *BUD4*, which codes for a large, novel protein (Bud4p) with a potential GTP-binding motif. Bud4p is expressed and localized to the mother/bud neck in all cell types. Most mitotic cells contain two apparent rings of Bud4 immunoreactive staining, as observed for Bud3p (Chant, J., M. Mischke, E. Mitchell, I. Herskowitz, and J. R. Pringle. 1995. *J. Cell Biol.* 129: 767–778). Early G1 cells contain a single ring of Bud4p immunoreactive staining, whereas cells at START and in S phase lack these rings. The level of Bud4p is also regulated in a cell cycle–dependent manner. Bud4p is inefficiently localized in *bud3* mutants and after a temperature shift of a temperature-sensitive mutant, *cdc12*, defective in the neck filaments. These observations suggest that Bud4p and Bud3p cooperate to recognize a spatial landmark (the neck filaments) during mitosis and support the hypothesis that they subsequently become a landmark for establishing the axial budding pattern in G1.

A VARIETY of cellular structures including cleavage furrows and septa need to be assembled at particular subcellular locations. Correct positioning of the division plane ensures that daughter cells inherit the appropriate complement of cellular components. Asymmetric placement of cleavage furrows and septa leads to asymmetric cell division, which can affect cell fate (Rhyu and Knoblich, 1995). The process of budding, a specialized form of cell division exhibited by the yeast *Saccharomyces cerevisiae*, requires restricted localization of molecules at the presumptive bud site. Both the cell division plane and the axis for cell polarity are determined by the choice of the site for budding. Analysis of bud-site selection provides an opportunity to study at a molecular level how a structure is assembled at a particular cellular location.

Initiation of bud growth involves several distinct molecular events. First, the appropriate site for budding must be recognized. Second, assembly of components required for bud formation occurs at that site. Third, the actin cytoskeleton and the secretory apparatus are oriented toward that site so that selective bud growth can occur (Drubin, 1991). The position of a new bud is dependent upon cell type (Hicks et al., 1977) and external factors, in particular, nutrient supply (Chant and Pringle, 1995; Thompson and Wheals, 1980; Gimeno et al., 1992; Madden and Snyder, 1992; Roberts and Fink, 1994). **a** or α cells grown in rich medium bud in an axial pattern, choosing new bud sites adjacent to the previous site of bud emergence (Chant and Pringle, 1995). In contrast, **a** or α cells at the bottom of a colony, presumably nutrient deprived, exhibit nonaxial budding (Roberts and Fink, 1994). **a**/α diploid cells grown in rich medium bud in a bipolar pattern, choosing new bud sites at either end of the cell (Chant and Pringle, 1995). When grown in nitrogen-poor solid medium, however, **a**/α diploids exhibit unipolar rather than bipolar budding (Gimeno et al., 1992; Kron et al., 1994).

Because cells displaying the axial pattern bud adjacent to the previous bud site (Chant and Pringle, 1995), an intracellular landmark that resides near the site of the previous cell division has been postulated to provide the cell with spatial memory (Chant and Herskowitz, 1991; Snyder et al., 1991). This landmark would be absent or nonfunctional in **a**/α diploid cells exhibiting the bipolar budding pattern. A candidate for this landmark is a cytoskeletal structure termed the 10-nm neck filaments, which assembles at the presumptive bud site about the time of bud emergence and persists until about the time of cytokinesis (Byers and Goetsch, 1976). Mutants defective in the *CDC3, CDC10, CDC11*, or *CDC12* genes lack these filaments and fail to undergo cytokinesis at restrictive temperatures (Hartwell, 1971; Longtine et al., 1996). *CDC3, CDC10, CDC11*, and *CDC12* encode a family of related proteins termed septins that contain a nucleotide-binding motif including a P loop and that are likely to be structural

Address all correspondence to S.L. Sanders, Department of Biochemistry and Biophysics, University of California, San Francisco, CA 94143-0448. Tel.: (415)476-4977. Fax: (415)502-5145. E-mail: sanders@cgl.ucsf.edu

components of the neck filaments (Ford and Pringle, 1991; Haarer and Pringle, 1987; Kim et al., 1991; Neufeld and Rubin, 1994; Flescher et al., 1993; Longtine et al., 1996). Genetic evidence supports the view that these filaments play a role in axial budding: mutations in any of these genes can affect the axial budding pattern (Chant et al., 1995; Flescher et al., 1993).

At least six genes (*BUD1/RSR1*, *BUD2*, *BUD3*, *BUD4*, *BUD5*, and *AXL1*) are required for **a** and α cells to exhibit an axial budding pattern (Bender and Pringle, 1989; Chant et al., 1991; Chant and Herskowitz, 1991; Fujita et al., 1994). Because mutations in *BUD3*, *BUD4*, and *AXL1* have a phenotype only in **a** and α cells, they are candidates for serving as or recognizing the axial landmark. The *AXL1* gene is expressed only in **a** and α cells and appears to be partially responsible for the difference in budding pattern exhibited by **a** and α vs **a**/α cells (Fujita et al., 1994). *AXL1* encodes a protein with similarity to insulin-degrading enzymes (Fujita et al., 1994), though its proteolytic activity seems not to be required for axial budding (Adames et al., 1995). Localization of Axl1p has not been reported. The Bud3 protein, whose sequence is novel, is present in all cell types and is localized in rings at the mother/bud neck for about half of the cell cycle (Chant et al., 1995). Localization of Bud3p to the mother/bud neck is dependent upon the integrity of the 10-nm neck filaments, suggesting that Bud3p recognizes the neck filaments as a morphogenetic landmark. After the neck filaments disappear at cytokinesis, Bud3p is positioned such that it could determine the location of the neck filaments in the next cell cycle (Chant et al., 1995).

To understand further the molecular basis of bud-site selection, we have characterized the *BUD4* gene and protein. We show here that *BUD4* encodes a large protein (Bud4p) with a potential GTP-binding motif at its carboxy terminus, whose levels are regulated in a cell cycle–dependent manner.

Immunofluorescence analyses revealed that Bud4p forms a ringlike structure that is localized to the mother/bud neck and that is present transiently after cytokinesis. Our data suggest that Bud3p and Bud4p cooperate to facilitate axial budding and support the hypothesis (Chant et al., 1995) that they participate in a cycle of protein–protein interactions to mark the bud site.

Materials and Methods

Materials

α-Factor, nocodazole, hydroxyurea, calcofluor, and polylysine were from Sigma Chem. Co. (St. Louis, MO). Fluorescent secondary antibodies were from Cappel (Malvern, PA). Horseradish peroxidase–coupled antibodies and Affi-Gel were from Bio-Rad Labs (Hercules, CA). Cyanogen bromide–activated Sepharose was from Pharmacia LKB Biotechnology (Piscataway, NJ), Clb2 antibodies were the kind gift of D. Kellogg, University of California (Santa Cruz, CA).

Microbiological and Molecular Biological Methods

Strains are described in Table I. Plasmids are described in Table II. DNA manipulations are described in Sambrook et al. (1989) and Ausubel et al. (1987) and yeast genetic methods in Rose et al. (1990). Synthetic low ammonium histidine dextrose (SLAHD) solid medium for pseudohyphal growth was prepared as described by Gimeno et al. (1992).

Budding Pattern Assays. Microcolony assays are described in Chant and Herskowitz (1991). Microcolonies of four cells were scored as axial when both mother and daughter cells budded proximally. Microcolonies of four cells were scored as bipolar when the daughter cell budded distally and the mother cell budded either proximally or distally. All other four-cell microcolonies were scored as random. Calcofluor staining is described in Pringle (1991). Cells with three or more adjacent bud scars were scored as axial. Cells with three or more bud scars clustered at the two cell poles were scored as bipolar. Cells with other staining patterns were scored as random.

α-Factor Arrest and Release. Synchronization with α-factor was essentially as described in Wittenberg et al. (1990). Cells were grown to early log phase ($OD_{600} \sim 0.3$) in YEPD. α-Factor was added to 10 μg/ml, and cells were incubated at 30°C for ~90 min. Cell cycle arrest was monitored by examining sonicated cells using Nomarski optics. After ~90% of the cells had accumulated without buds, samples were taken for analysis of G1-arrested cultures. The remaining cells were washed twice with 30°C YEPD and returned to growth. Samples taken every 10–15 min were fixed for immunofluorescence and budding index determination or lysed for immunoblot analysis.

Nocodazole and Hydroxyurea Treatment. Cells were grown to early log phase in YEPD and treated with 10 μg/ml nocodazole dissolved in DMSO, DMSO alone, 0.2 M hydroxyurea dissolved in water, or water alone (Jacobs et al., 1988; Slater, 1973). Cells were incubated for ~90 min at 30°C. Cell cycle arrest was assessed by examining sonicated cells using Nomarski optics. When at least 70% of the nocodazole- or hydroxyurea-treated cells had attained a large-budded cell morphology, samples were fixed for immunofluorescence or lysed for immunoblot analysis.

G1 Cyclin Shut-off. Cells of strain ASY80 (*Δcln1 Δcln2 Δcln3 pGAL::CLN2*) or wild-type cells in the same background (JO369) were grown to early log phase in YEP-galactose medium. An aliquot of each strain was shifted into YEP-glucose medium for 3.5 h to shut off the *GAL* promoter and to deplete ASY80 of Cln2p. Samples were then prepared for immunoblot analysis.

Nutrient Deprivation. Cells were grown from early log phase ($OD_{600} \sim 0.3$) to late log phase ($OD_{600} \sim 10$). Samples were taken approximately every 2 h for budding index determination and immunoblot analysis.

cdc12-6 Temperature-shift. *cdc12-6* strains containing either YCp50 or YEp24*CDC12* were grown to early log phase at 25°C in minimal medium lacking uracil and treated with nocodazole as described above. After treatment, cells were split into two aliquots, one incubated at 37°C for 10 min, the other at 25°C. Samples were then fixed and prepared for immunofluorescence.

Cloning of BUD4

SY59 (**a** *bud4-1 ura3*) was transformed with a yeast library (Carlson and Botstein, 1982). Approximately 11,000 transformants were patched onto SLAHD plates in two concentric rings of 25 (because the pseudohyphal phenotype in **a** and α cells was sensitive to position on the plate as well as the number of colonies per plate).

Plates were incubated for 2 wk at 30°C and scored for pseudohyphae by microscopic examination at 30× magnification. Colonies that failed to form pseudohyphae were retested and assayed for budding pattern. Plasmid DNA was isolated from the five colonies that exhibited axial budding. These were shown to be identical by restriction analysis. One plasmid so identified, p*BUD4*, was shown to contain *BUD4* as follows: The p*BUD4* DNA insert was cloned into pRS306, a yeast integrating vector containing *URA3* (Sikorski and Hieter, 1989). The resultant plasmid, pSS10, was linearized with SalI and used to transform IH2390 (α *BUD4 ura3-52*) to uracil prototrophy, thus marking the locus with *URA3*. Integration of the plasmid at the correct locus was confirmed by Southern analysis (data not shown). The resultant strain, SY127, was crossed to IH2410 (**a** *bud4-1*), and the meiotic progeny analyzed. In 44 of 45 tetrads (from two independent diploids) the Bud^+ phenotype segregated 2:2. All Bud^+ progeny were Ura^+, and all Bud^- progeny were Ura^-. In the exceptional tetrad, uracil prototrophy segregated 2:2 whereas the budding phenotype segregated 3 Bud^+:1 Bud^-, probably due to gene conversion. These data indicate that the p*BUD4* plasmid carries the authentic *BUD4* gene.

Sequencing of BUD4

Subclones of *BUD4* were prepared in pBLUESCRIPT (Stratagene, LaJolla, CA). A set of nested deletions was prepared by exonuclease III digestion (Henikoff, 1984) using the Exo-Size Deletion Kit (New England BioLabs, Inc., Beverly, MA). Deletion clones on the coding strand were sequenced by the dideoxy method (Sanger et al., 1977) using the USB™

Table I. Yeast Strains Used in This Study

Strain	Genotype	Source
SY59	**a** *ura3-52 bud4-1*, product of a cross between IH2410 and CG146	This study
IH2390	α *HMRα HMLα his4 trp1 ura3 can1 MAL2*	Chant and Herskowitz, 1991
SY127*	*bud4::BUD4-URA3*	This study
SY298*	*bud4::TRP1*	This study
SY299*	**a** *bud4::TRP1*	This study
SY300*	**a**/α *bud4::TRP1/bud4::TRP1*	This study
IH2393*	**a**	Chant and Herskowitz, 1991
IH2407*	**a** *bud1-1*	Chant and Herskowitz, 1991
IH2408*	**a** *bud2-1*	Chant and Herskowitz, 1991
IH2409*	**a** *bud3-1*	Chant and Herskowitz, 1991
IH2410*	**a** *bud4-1*	Chant and Herskowitz, 1991
IH2424*	**a** *bud5::URA3*	Chant and Herskowitz, 1991
SY401*	**a** *axl1::URA3*	This study
MM5.1*	**a** *bud3::URA3*	Chant et al., 1995
IH2397*	**a**/α	Chant and Herskowitz, 1991
JO31-1A	**a** *ade2-101 ura3-52 lys2-801^a his3-Δ200 leu2-Δ1 trp1-Δ63*	Herskowitz lab collection
JO13‡	α	Herskowitz lab collection
JO292‡	**a**/α	Herskowitz lab collection
SY294‡	**a** *bud4::LEU2*	This study
CGX69	**a**/α *ura3-52/ura3-52*	Gimeno et al., 1992
CG146	α *ura3-52*	Gimeno et al., 1992
JO369	**a** *ade2-101° ura3-52 lys2-801^a his3-Δ200 leu2-Δ1 Gal2$^+$*	J. Ogas
ASY80§	α *cln1::TRP1 cln2::LEU2 cln3::TRP1 pGAL-CLN2-HIS3*	A. Sil
SY283	**a** *cdc12-6 ura3-52 his4*	J. R. Pringle lab collection and this study

*Isogenic to IH2390 except where noted.
‡Isogenic to JO31-1A except where noted.
§Isogenic to JO369 except where noted.

Sequenase™ Version 2.0 Sequencing Kit. The noncoding strand was sequenced by the UCSF Biomedical Resource Center (San Francisco, CA). Primers were designed to fill in gaps after the deletions were analyzed. The *BUD4* sequence has been submitted to GenBank, accession No. U41641. The yeast genome project has also revealed an ORF, YJR092w, that is probably the *BUD4* gene, which has eight nucleotide differences from GenBank U41641: Three of these differences were single nucleotide additions in the YJR092w sequence after nucleotides 361, 528, and 589, respectively, of the U41641 sequence. Reinspection of this region revealed that YJR092w is identical to U41641 in this region (Massoud Ramezani Rad, Institut fur Mikrobiologie, Dusseldorf, Germany, personal communication). In addition, YJR092w has an A insert after positions 1143, 1185, and 1258 of the U41641 sequence; T1294 and A3677 of the U41641 sequence correspond to A and G, respectively, in the YJR092w sequence. The two amino acid sequences are therefore identical between amino acids 1 and 380, from amino acids 432 to 1225, and from amino acid 1227 until the end (using the numbering system of U41641).

Deletion of the BUD4 Gene

The *BUD4* coding sequence in plasmid pSS24 was replaced with either *LEU2* or *TRP1*. pSS24 was digested with AgeI (which cuts 30 nucleotides upstream of the translation termination codon) and filled in with the large fragment of *E. coli* DNA polymerase I (Klenow) (New England Biolabs). The plasmid was then digested with SphI, which cuts at the initiator ATG of the *BUD4* open reading frame (ORF)[1], and then treated with T4 3′-5′ exonuclease (New England Biolabs). SalI linkers were ligated onto the resultant blunt ends and the vector recircularized. This plasmid, pSS36, lacked *BUD4* sequences from the first ATG of the predicted open reading frame but contained the carboxy-terminal nine codons. The ~2.2-kb SalI fragment of *LEU2* from pLK9 was ligated into the SalI site of pSS36, resulting in pSS38. The ~1-kb HincII/StuI fragment of *TRP1* from YPP14 was cloned into the SalI site of pSS36 that had been filled in with the Klenow fragment of *E. coli* DNA polymerase I to create pSS42. *BUD4* was disrupted in **a**, α, and **a**/α cells of two strain backgrounds. To disrupt *BUD4* in the S288C background, pSS38 was digested with BglII and BamHI, and JO31-1A (**a**), JO13 (α), and JO292 (**a**/α) strains were transformed to leucine prototrophy. To disrupt *BUD4* in a strain background used in previous bud-site selection studies (Chant and Herskowitz, 1991), pSS42 was digested with AflII, and IH2390 (α), IH2393 (**a**), and IH2397 (**a**/α) strains were transformed to tryptophan prototrophy. Genomic DNA was prepared from these strains, digested with BstXI, and analyzed by Southern blotting using the ~0.5-kb BstXI–SphI fragment as the probe, which confirmed that the *BUD4* gene was disrupted (data not shown).

1. Abbreviations used in this paper: ORF, open reading frame; GST, glutathione-*S*-transferase.

Preparation of Bud4p Antiserum

Preparation of a Glutathione-S-Transferase Fusion Protein. To create an in-frame fusion of glutathione-*S*-transferase to the NH_2-terminal ~36-kD of Bud4p, pSS15 was digested with SphI and treated with T4 3′-5′ exonuclease followed by digestion with BglII. This ~1.2-kb SphI/BglII fragment was cloned into pGEX1* (pGEX from Pharmacia modified by K. Oegema, UCSF, San Francisco, CA) that had been digested with KpnI and treated with T4 3′-5′ exonuclease followed by digestion with BglII. The resultant plasmid, pSS43, was transformed into a protease-deficient *E. coli* strain, NB42 (a gift from Peter Jackson, Stanford University). The fusion protein was purified using glutathione affinity chromatography (Kellogg et al., 1995). One liter of LB containing 100 μg/ml carbenicillin was grown to OD_{600} 0.49, at which time IPTG was added to 0.8 mM, and the culture grown for 195 min to OD_{600} 1.9. Cells were harvested, washed with PBS, and frozen in liquid nitrogen. Pellets were thawed in 1× PBS containing 1 mM EGTA, 1 mM EDTA, 2 mM benzamidine, 200 μg/ml lysozyme, and 1 mM PMSF (lysis buffer). The suspension was sonicated three times for 15 s using a Branson Sonifier Cell Disruptor 185 fitted with a microtip, and then clarified by centrifugation at 10,000 rpm in an SS34 rotor for 60 min at 4°C. The lysate was treated with 10 μg/ml RNase I and 10 μg/ml DNase I for 5 min at 4°C and again clarified. The supernatant was applied at ~0.4 ml/min to a 1-ml glutathione agarose column equilibrated with 1× PBS, and the flow-through reapplied to the column. The column was then

Table II. Plasmids Used in This Study

Plasmid name	Description	Source
p*BUD4*	Original *BUD4* complementing clone	This study
pSS1	SalI fragment of p*BUD4* in the SalI site of YEp24	This study
pSS2	p*BUD4* lacking SalI fragment	This study
pSS3	SphI fragment of p*BUD4* in the SphI site of YEp24	This study
pSS7	SphI–BamHI fragment of p*BUD4* in the SphI–Bam HI sites of YEp24	This study This study
pSS8	XbaI fragment of p*BUD4* in the NheI site of YEp24	This study
pSS9	SphI–BamHI fragment of p*BUD4* in the SphI–BamHI sites of YCp50	This study
pSS10	XhoI–BamHI fragment of p*BUD4* in the XhoI–BamHI sites of pRS306	This study
pSS15	entire p*BUD4* insert (recreated by cloning the 4-kB SalI fragment and the ~7-kB SalI–SmaI fragments into the SalI and SmaI sites) in pBLUESCRIPT	This study
pSS17	PvuII fragment of pSS15 in the PvuII site of YEp24	This study
pSS18	PvuII fragment of pSS15 in the HpaI site of YCp50	This study
pSS24	pSS15 lacking the MluI/KpnI fragment	This study
YEp24CDC12	2 μ *CDC12*	H. Fares and J. Pringle, UNC
pLK9	SalI fragment of *LEU2* in pUC8	J. Li, UCSF
YPP14	HincII fragment of *TRP1* in pUC8	J. Li, UCSF
pSS36	SphI–AgeI fragment of pSS24 replaced with SalI linkers	This study
pSS38	SalI fragment of *LEU2* cloned into the SalI site of pSS36	This study
pSS42	HincII–StuI fragment of *TRP1* cloned into the SalI site of pSS36	This study
pSS43	SphI (chewed back)–BglII fragment of pSS15 in the KpnI (filled-in)-BglII site of pGEX*	This study
pGEX1*	pGEX with an altered polylinker	K. Oegema, UCSF

washed with 40 ml lysis buffer containing 0.5 mM DTT and 0.1% Tween 20 and subsequently washed with lysis buffer containing 0.5 mM DTT until no protein detectable by Bradford assay (Bio-Rad) leached off the column. The fusion protein was eluted with lysis buffer containing 1 mM DTT and 5 mM glutathione. Fractions containing protein were pooled and concentrated with a Centriprep 30, yielding 11.3 mg protein. 0.5 mg protein was used for the initial injection of two rabbits and for subsequent boosts (Berkeley Antibody Company [BAbCO], Richmond, CA).

Antibody Purification. Crude serum was adsorbed against a cyanogen bromide–activated Sepharose column coupled to a bacterial extract derived from cells expressing glutathione-*S*-transferase. The flow-through from this column was applied to a cyanogen bromide–activated Sepharose column coupled to a yeast extract derived from strain SY298 (α *bud4::TRP1*). The flow-through from the second column was applied to an Affi-Gel 10 column coupled to the Bud4p-GST fusion protein. Antibodies were eluted with 0.2 M glycine, pH 2.2. Fractions were collected and immediately neutralized with 3 M Tris, pH 9. Protein-containing fractions were identified using the Bradford assay, pooled, and adjusted to 50 mM Hepes, pH 6.8, 1 mg/ml BSA, and 5 mM NaN_3. The affinity-purified antibody was stored at −80°C and the working stock at 4°C.

Immunofluorescence

The protocol was essentially that of Pringle et al. (1991). Cells were grown to early to mid log phase, fixed with formaldehyde for 1–16 h, collected by centrifugation, washed with phosphate buffer, and then spheroplasted.

Spheroplasts were applied to polylysine-coated slides and further permeabilized by treatment with 0.2% SDS in 1× PBS (Ziman, 1993), followed by submersion in −20°C methanol for 6 min and in −20°C acetone for 30 s (Novick and Botstein, 1985). Bud4 antibody was used at a 1:5 dilution. The secondary antibody was fluorescein-conjugated anti rabbit–IgG antibody.

Cell Extracts and Western Blots

Cells were grown to early to mid log phase, collected by centrifugation, washed with water, and resuspended in 50 mM Tris, pH 7.5, 1% SDS, 5 mM DTT, 1 mM EDTA, and 1 mM PMSF. Samples were heated to 95°C, mixed with glass beads, and vortexed three times for 30 s. Protein concentration was determined (Markwell et al., 1978) and all samples adjusted to the concentration of the most dilute sample. Samples (typically ~150 μg protein) were fractionated using 6% SDS-polyacrylamide mini-gels, and proteins transferred to nitrocellulose filters in 150 mM glycine, 20 mM Tris, pH 7.5, 20% methanol, 0.05% SDS. Filters were blocked for 1–16 h in TBS containing 0.1% Triton X-100 and 2% nonfat dry milk and decorated with a 1:500 dilution of the affinity-purified Bud4p antibodies. Bud4 protein was visualized using the Amersham ECL protein detection kit.

Printing and Photography

Cells were visualized with a Zeiss Axioskop and photographed with TMAX 400 film (ASA set at 1600). Images were printed on Rapitone P1-4 paper and arranged using Adobe Photoshop.

Results

Use of the Pseudohyphal Behavior of bud4 Mutants to Clone BUD4

The ability of yeast cells to exhibit pseudohyphal growth is correlated with the bipolar budding pattern. **a**/α diploids, which exhibit bipolar budding, form pseudohyphae in certain strain backgrounds when starved for nitrogen (Gimeno et al., 1992). **a** and α cells, which exhibit the axial budding pattern, do not form pseudohyphae, nor do **a**/α diploids that exhibit random budding due to a mutation in *BUD1*. To test whether a bipolar budding pattern allows cells to form pseudohyphae, the behavior of **a** *bud4* and α *bud4* mutants, which exhibit bipolar budding, was examined. The *bud4-1* mutation in IH2410 (Chant and Herskowitz, 1991) was introduced into a strain background (CG146) suitable for scoring pseudohyphal growth (Gimeno et al., 1992). Two of 21 of the *bud4-1* haploid segregants from this cross, including SY59, exhibited pseudohyphal growth (Fig. 1 *c*). The low fraction of *bud4-1*

progeny exhibiting this behavior indicates that additional genes important for pseudohyphal development segregated in these crosses. These results demonstrated that the *bud4-1* mutation could indeed allow **a** and α haploids to form pseudohyphae in the appropriate strain background.

The *BUD4* gene was cloned by screening for reversal of the pseudohyphal growth behavior of *bud4-1* strain SY59. Pseudohyphal growth was assessed by observing the morphology of a colony edge using a dissecting microscope (Fig. 1). Although the pseudohyphae formed by α *bud4-1* strains were not as long as those of **a**/α *Bud*$^+$ strains (Fig. 1, compare *b* and *c*), it was possible to distinguish α *bud4-1* and α *BUD4* strains (Fig. 1, compare *a* and *c*). SY59 was transformed with a yeast genomic library (Carlson and Botstein, 1982), and ~11,000 transformants were patched onto SLAHD plates. 83 reproducibly failed to form pseudohyphae (Fig. 1 *d*). Five of these exhibited axial budding and contained identical plasmids (data not shown). Genetic analysis showed that the ~11-kb insert mapped to the *BUD4* locus (see Materials and Methods). Most subclones failed to complement (Fig. 2 *A*), consistent with the existence of a single long open reading frame (Fig. 2 *A*, row *g*). *BUD4* has the potential to encode a protein, Bud4p, of 1,446 amino acids (data not shown) with a putative GTP-binding site at its carboxy terminus (Fig. 2 *B*). Bud4p lacks hallmark sequences of any particular subfamily of GTPases (Bourne et al., 1991). In addition, the presumptive upstream regulatory region of *BUD4* contained a sequence that may confer cell cycle–dependent transcription: the segments from −206 to −154 is similar to the promoter segment of *SWI5* and *CLB2* that are necessary and sufficient to restrict transcription to the late S, G2, and M phases of the cell cycle (Fig. 2 *C*) (Lydall et al., 1991; Maher et al., 1995). The *BUD4* upstream region is also similar to the presumptive regulatory region of *BUD3*, suggesting that *BUD3*, *BUD4* and perhaps *SWI5* and *CLB2* are coordinately regulated.

BUD4 Null Phenotype

BUD4 null alleles were constructed by replacing all coding information except the nine carboxy-terminal codons with *LEU2* or *TRP1* (see Materials and Methods) (Rothstein, 1983). These *bud4::LEU2* and *bud4::TRP1* alleles (Fig. 2 *A*, rows *h* and *i*) were then used to replace the genomic *BUD4* in two strain backgrounds. Gene replacement was

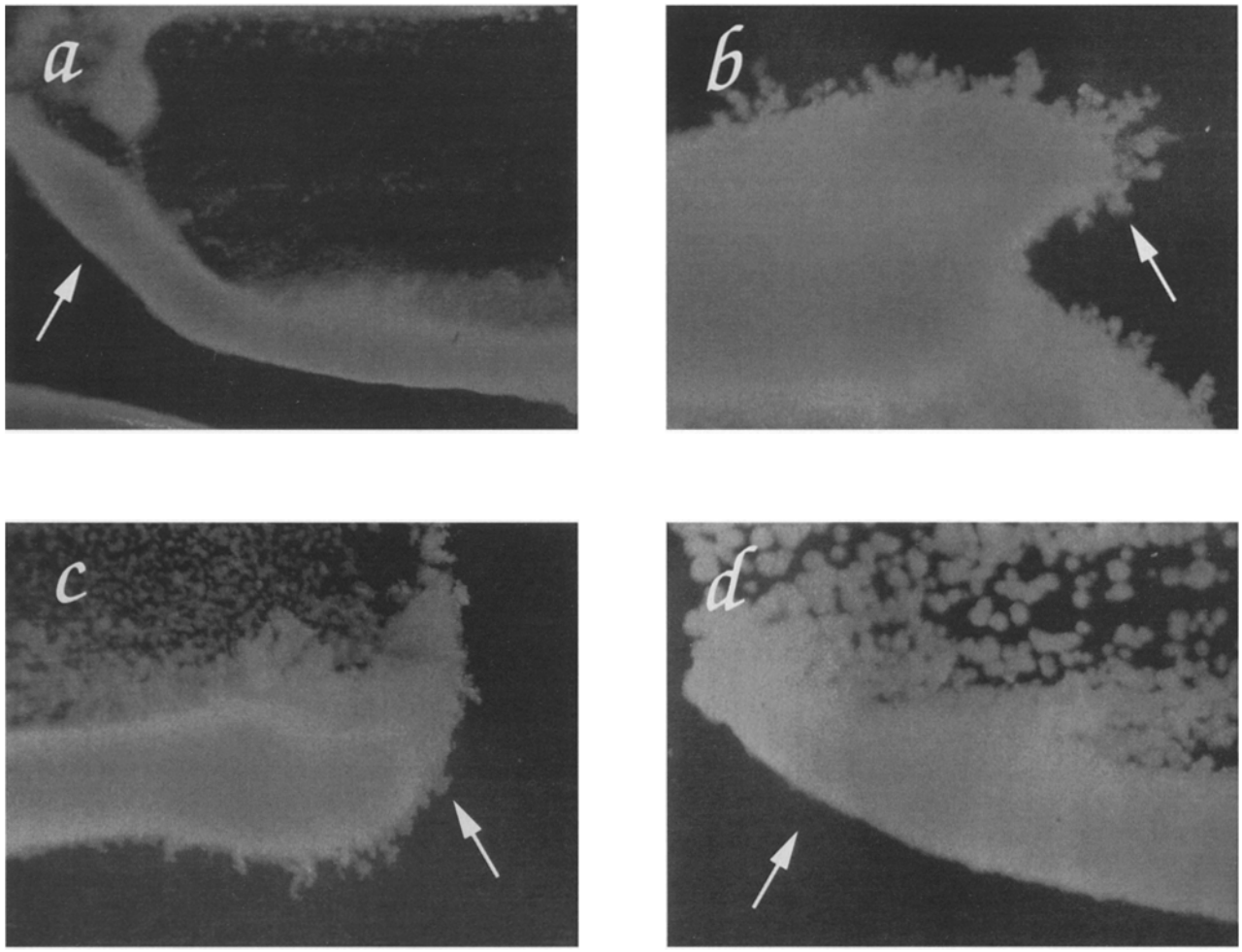

Figure 1. Cloning of *BUD4*, which encodes a potential GTP-binding protein, by reversal of pseudohyphal growth behavior. CG146 (α *Bud*$^+$) containing YEp24 (*a*), CGX69 (**a**/α *Bud*$^+$) containing YEp24 (*b*), SY59 (α *bud4-1*) containing YEp24 (*c*), or SY59 containing p*BUD4* (*d*) were patched onto SLAHD solid medium and incubated for two weeks at 30°C. Arrows indicate positions of patch edges.

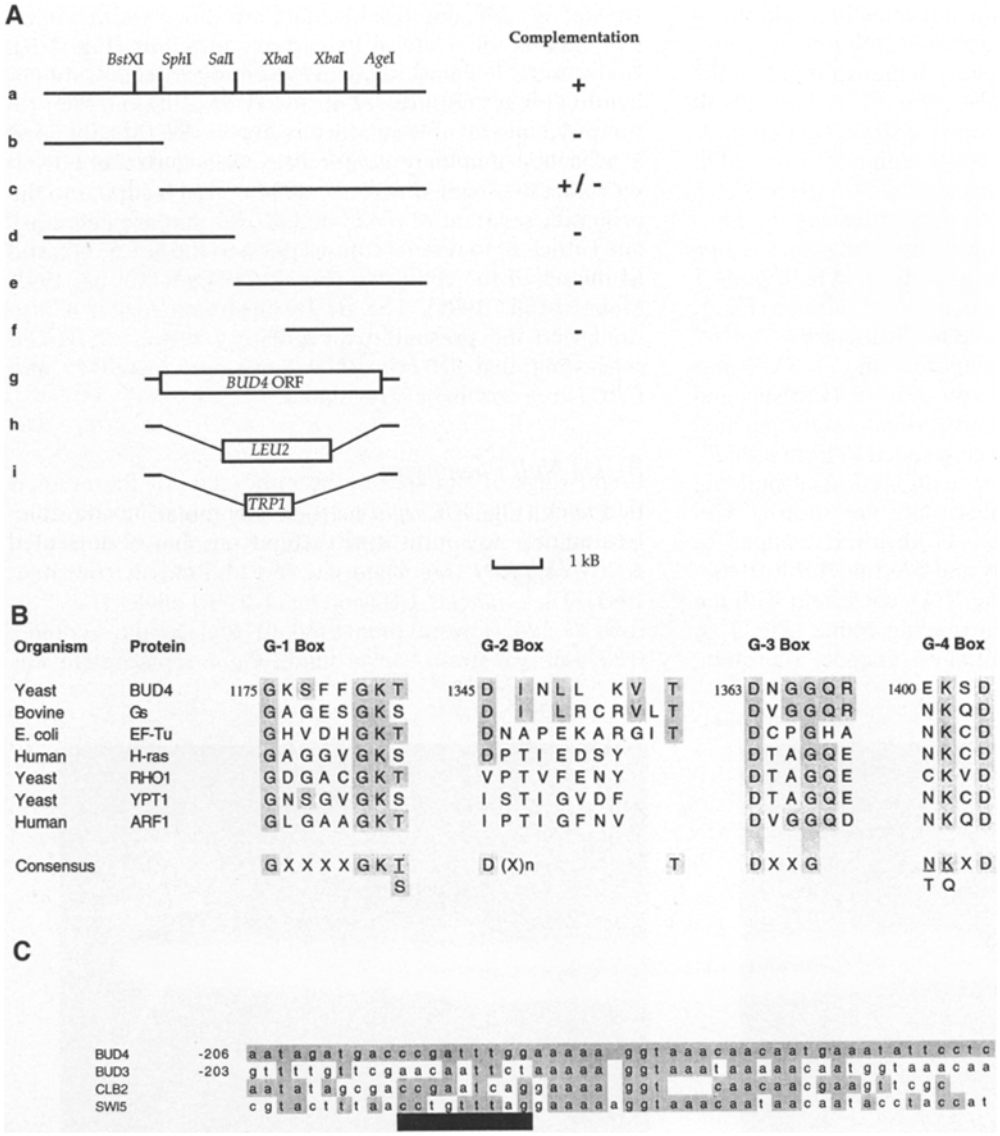

Figure 2. BUD4 encodes a putative cell cycle–regulated GTPase. (*A*) Restriction map of the *BUD4* locus (*a*), and subclones (pSS3, *b*; pSS7 [in YEp24] and pSS9 [in YCp50], *c*; pSS1, *d*; pSS2, *e*; pSS8, *f*), position of the *BUD4* ORF (*g*), and *BUD4* deletion constructs (*h* and *i*). "+" designates clones with complementing activity; "−" designates clones lacking complementing activity, and "±" designates a clone that could complement the budding defect of *bud4-1* when present in YEp24 but not in YCp50. (*B*) Comparison of Bud4p to conserved sequences in a variety of known GTPases (Bobak et al., 1989; Gallwitz et al., 1983; Laursen et al., 1981; Madaule et al., 1987; Capon et al., 1983; Robishaw et al., 1986) and to the consensus sequence (Bourne et al., 1991). (*C*) Comparison of upstream nucleotide sequences of *BUD4* to the upstream regulatory sequences of *SWI5* and *CLB2* that are necessary and sufficient for proper cell cycle–regulated transcription (Lydall et al., 1991; Maher et al., 1995) and to the upstream sequences of *BUD3* (Chant et al., 1995). An Mcm1p-binding site is underscored in black (Kuo and Grayhack, 1994).

confirmed by Southern analysis (see Materials and Methods). **a**, α, and **a**/α cells lacking *BUD4* exhibited a bipolar pattern like that of the original *bud4-1* mutant (Table III). Growth of **a**, α, and **a**/α strains lacking *BUD4* was normal at all temperatures, on rich and minimal media, and on media with a variety of carbon sources or increased osmolarity. Sporulation efficiency and spore morphology were unaffected by loss of the *BUD4* gene. A modest reduction in efficiency of mating was observed in α cells of the S288C strain background by qualitative patch mating tests (data not shown); the significance of this reduction remains to be tested. As observed for *BUD1*, *BUD2*, *BUD3*, and *BUD5* (Bender and Pringle, 1989; Chant et al., 1991; Chant et al., 1995; Park et al., 1993), all existing evidence suggests that the primary role of *BUD4* in an otherwise wild-type cell is to facilitate appropriate bud-site selection.

Bud4p Localizes to the Mother/Bud Neck

To determine the subcellular localization of Bud4p, it was necessary to generate polyclonal antibodies against Bud4p. A fusion protein composed of the NH_2-terminal 36-kD of Bud4p (see Materials and Methods) and glutathione-*S*-transferase was prepared as antigen. Polyclonal antisera from two rabbits recognized a protein of apparent molecular mass 230 kD present in wild-type (*BUD4*) extracts and absent from *bud4::TRP1* extracts (Fig. 3 *A*). The sequence of the *BUD4* gene predicts a protein with a molecular mass of ~170 kD. The 230-kD polypeptide was identified as Bud4p because it was overexpressed in extracts from cells carrying *BUD4* on a high copy plasmid (data not shown) and because it exhibited greater mobility on SDS-PAGE when derived from extracts from a *bud4-1* mutant (Fig. 7 *B*). Many proteins, particularly those that do not have globular structures, exhibit SDS-PAGE mobilities slower than predicted from their sequence (for example see Field and Alberts, 1995).

Affinity-purified polyclonal antiserum was used to stain fixed spheroplasts by indirect immunofluorescence. Cells deleted for *BUD4* exhibited a diffuse haze throughout the mother and the bud (Fig. 3 *B*, column *c*). Analysis of several hundred wild-type cells stained with Bud4 antibodies

Table III. Phenotype of a bud4 Null Mutant

Relevant genotype	Axial	Bipolar	Random	Total
α *BUD* (IH2390)	281	15	4	300
α *bud4::TRP1* (SY298)	72	215	13	300
a *BUD* (IH2393)	266	28	6	300
a *bud4::TRP1* (SY299)	78	210	12	300
a *bud4-1* (IH2410)	81	206	13	300
BUD/BUD **a**/α (IH2397)	46	248	17	301
bud4::TRP1/ *bud4::TRP1* **a**/α (SY300)	32	263	15	300

Microcolony budding assays were performed to determine the budding pattern of isogenic strains.

revealed two classes of staining. 30–50% of unbudded cells exhibited an apparent ring of staining (Fig. 3 *B*, column *a*). Approximately fifty percent of budded cells contained two apparent rings of staining (Fig. 3 *B*, column *b*). The rings were located on either side of the mother/bud neck, with one ring present in the mother cell and one ring in the bud. Cells with small buds were unstained (data not shown).

Presence and Localization of Bud4p Are Cell Cycle–dependent

The observations of Bud4p localization in asynchronous cultures suggested that the localization of Bud4p was cell cycle–dependent. We tested this hypothesis directly using synchronous populations of cells. Cells arrested in mitosis by addition of nocodazole accumulated more Bud4p than cells in asynchronous cultures (Fig. 4 *A*, compare lane *1* to lanes *2–4*). In contrast, cells arrested with hydroxyurea accumulated less Bud4p than did asynchronous cultures (Fig. 4 *A*, compare lane *1* to lanes *5–8*). The immunofluorescence data paralleled these observations: 78% (n = 100) of cells arrested with hydroxyurea contained two faint rings of Bud4p that were localized to either side of the mother/bud neck (Fig. 4 *B*, *left panels*). 92% (n = 100) of cells arrested in mitosis with nocodazole contained two bright rings of Bud4p, one on either side of the mother/bud neck (Fig. 4 *B*, *right panels*). Staining of nocodazole-treated cells was indistinguishable from that of untreated cells with buds of similar size (compare Fig. 4 *B*, *right panels* to Fig. 3 *B*, column *b*).

Bud4p was also examined in cells arrested in G1. First, cells were arrested at START by depletion of G1 cyclins (Richardson et al., 1989; Nasmyth, 1993). Strain ASY80 lacks chromosomal copies of *CLN1*, *CLN2*, and *CLN3* and is kept alive by expression of *CLN2* from a galactose-regulated *CLN2* gene. When grown in galactose, these cells exhibit near normal morphology and cell division. When shifted into glucose-containing medium, unbudded cells accumulate (Sil, A., personal communication, Fig. 5 *A*). We observed that ASY80 cells grown in galactose-containing medium contained Bud4 protein (Fig. 5 *A*, lane *3*),

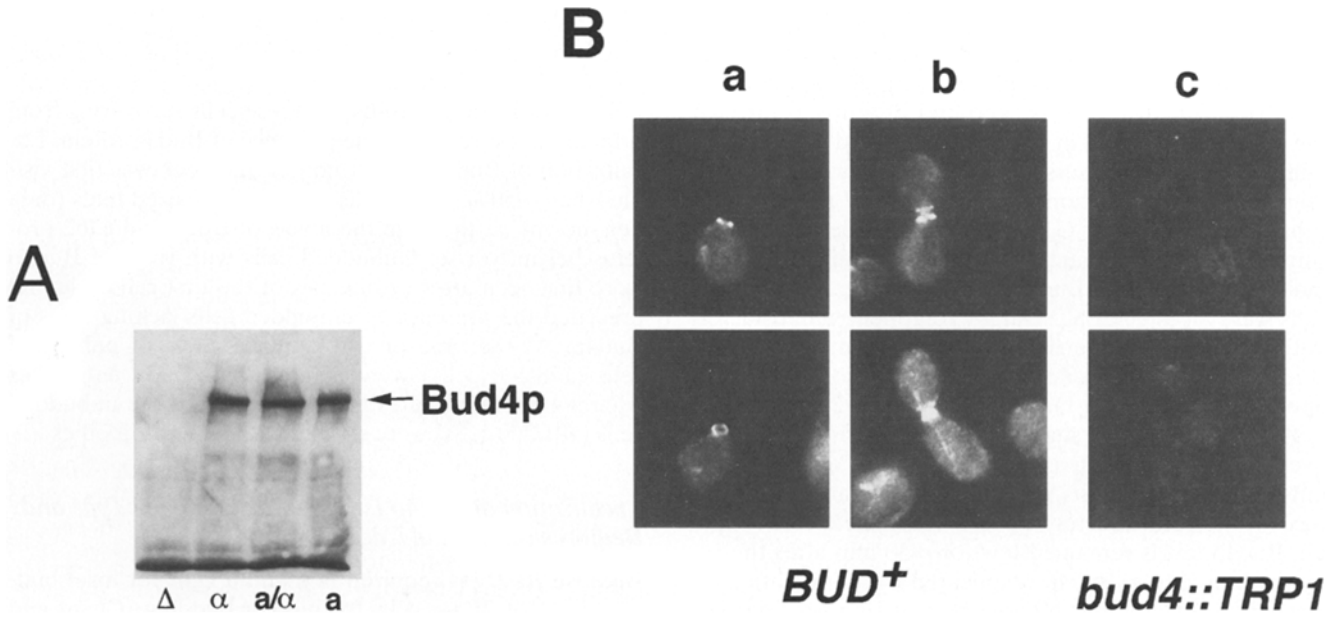

Figure 3. Identification and localization of Bud4 protein. (*A*) Extracts derived from cells of isogenic strains SY298 (α *bud4::TRP1*), IH2390 (α *BUD*), IH2397 (**a**/α *BUD*), and IH2393 (**a** *BUD*) were analyzed for Bud4p by immunoblotting. The band at the dye front is a cross-reacting protein which, as shown, is also present in *BUD4* deletion extracts. Equal amounts of protein were loaded in each lane. (*B*) Cells of isogenic strains IH2393 (**a** *BUD*) (columns *a* and *b*) and SY299 (**a** *bud4::TRP1*) (column *c*) were grown to early log phase, fixed, and processed for indirect immunofluorescence staining with affinity-purified Bud4p antibodies.

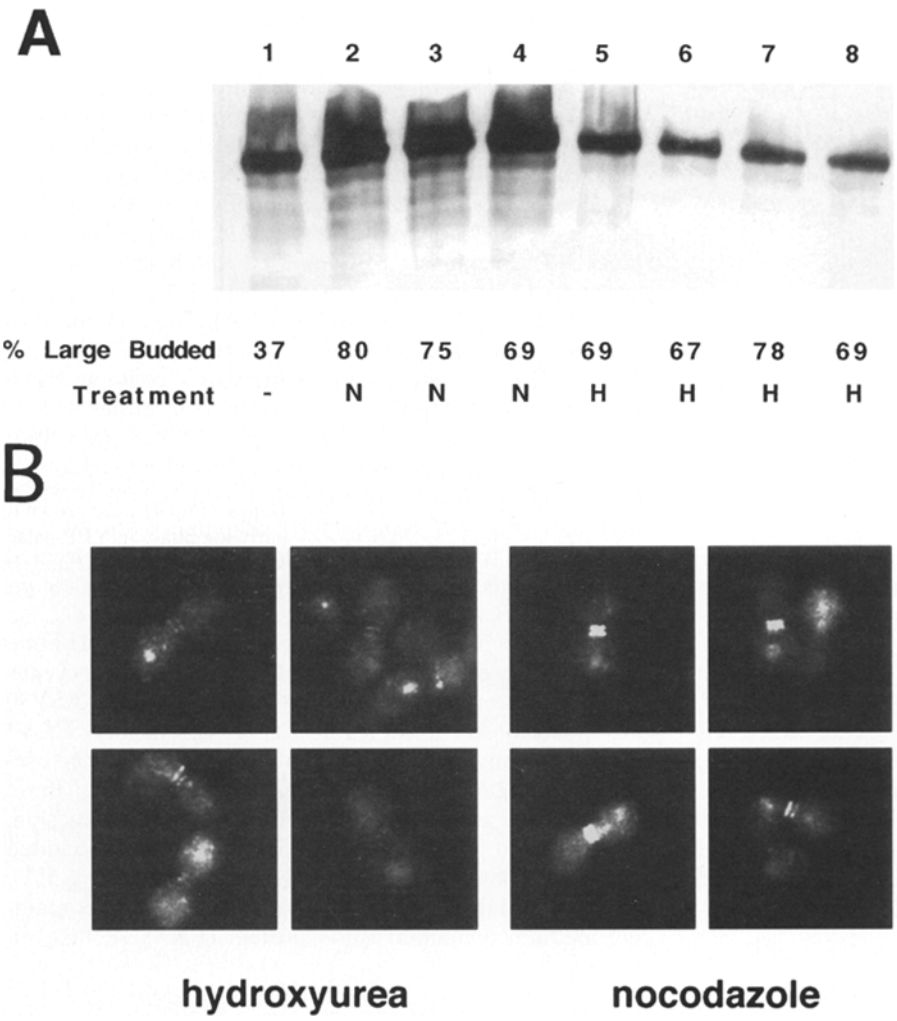

Figure 4. Presence and localization of Bud4p in cells arrested in S and M phases of the cell cycle. (*A*) Extracts were derived from cells of strain IH2393 (**a** *BUD4*) grown to early log phase and mock treated (lane *1*), treated with nocodazole at 5 μg/ml (lane *2*), 10 μg/ml (lane *3*), or 20 μg/ml (lane *4*), or with hydroxyurea at 10 mM (lane *5*), 20 mM (lane *6*), 40 mM (lane *7*), or 80 mM (lane *8*) for 2 h at 30°C, and then analyzed for Bud4p by immunoblotting. Arrest of cells was analyzed by examining cell morphology; percent arrested cells is indicated below the corresponding lanes. Equal amounts of protein were loaded in each lane. (*B*) Cells of strain IH2393 (**a** *BUD4*) were grown to early log phase, treated with 0.2 M hydroxyurea (*left panels*) or 10 μg/ml nocodazole (*right panels*) as described in *A*, fixed, and processed for indirect immunofluorescence staining with affinity-purified Bud4p antibodies.

whereas ASY80 cells shifted into glucose-containing medium possessed little Bud4 protein (Fig. 5 *A*, lane *4*). A Cln^+ strain in the same background progressed through the cell cycle normally in both galactose- and glucose-containing media and possessed similar amounts of Bud4 protein under both conditions (Fig. 5 *A*, lanes *1* and *2*). Next, cells were arrested at G1/G0 by nutrient depletion (Nasmyth, 1993). As cell number increased, both the budding index and the level of Bud4p decreased (Fig. 5 *B*). Finally, cells were arrested at START by treatment with α-factor. Although **a** cells in asynchronous cultures contained Bud4p (Fig. 5 *C*, lane *1*, *top panel*), Bud4p levels dropped sharply upon treatment with α-factor (Fig. 5 *C*, lane *2*).

These observations suggested that Bud4p levels varied over the cell cycle with a trough at START and a peak in mitosis. This hypothesis was confirmed by analyzing cells recovering from α-factor–induced cell cycle arrest (Fig. 5 *C*). Bud4p levels remained low for ~30 min after the removal of α-factor. Bud4p reappeared by 40 min after release from α-factor, just before entry into mitosis (Fig. 5 *C*, lanes *6* and *7*). The timing of mitosis was determined by immunoblot analysis of Clb2p, a mitotic B-type cyclin (Fitch et al., 1992; Richardson et al., 1992; Grandin and Reed, 1993; Surana et al., 1991, Ghiara et al., 1991), and by examination of bud sizes. The pattern of reappearance of Bud4p nearly paralleled that of Clb2p (Fig. 5 *C*, *lower panel*) (Grandin and Reed, 1993).

The localization of Bud4p in these cells recovering from α-factor arrest reflected the presence of Bud4 protein. Localization of Bud4p to the mother/bud neck was first visible when ~50% of the cells had medium-sized buds (data not shown), at the time the levels of Bud4 and Clb2 proteins began to rise. Unbudded cells with rings of Bud4p were first seen after cytokinesis of the first cell cycle and preceded the presence of unbudded cells lacking rings of Bud4p. At the time of cytokinesis, ~90% of unbudded cells (178/200 cells) were stained with Bud4 antibodies whereas fifteen minutes later, only half of the unbudded cells (101/200 cells) were stained with Bud4 antibodies.

Localization of Bud4p Is Independent of Cell Type and Requires Bud3p and Cdc12p

Because *BUD4* is required in **a** and α cells for axial budding but not in **a**/α cells for bipolar budding (Chant and Herskowitz, 1991), it was of interest to determine whether **a**/α cells synthesize Bud4p. Bud4 protein was present at similar levels and exhibited the same apparent molecular weight in **a**, α, and **a**/α cells (Fig. 3 *A*). Localization of Bud4p was identical in all cell types as well (Fig. 6).

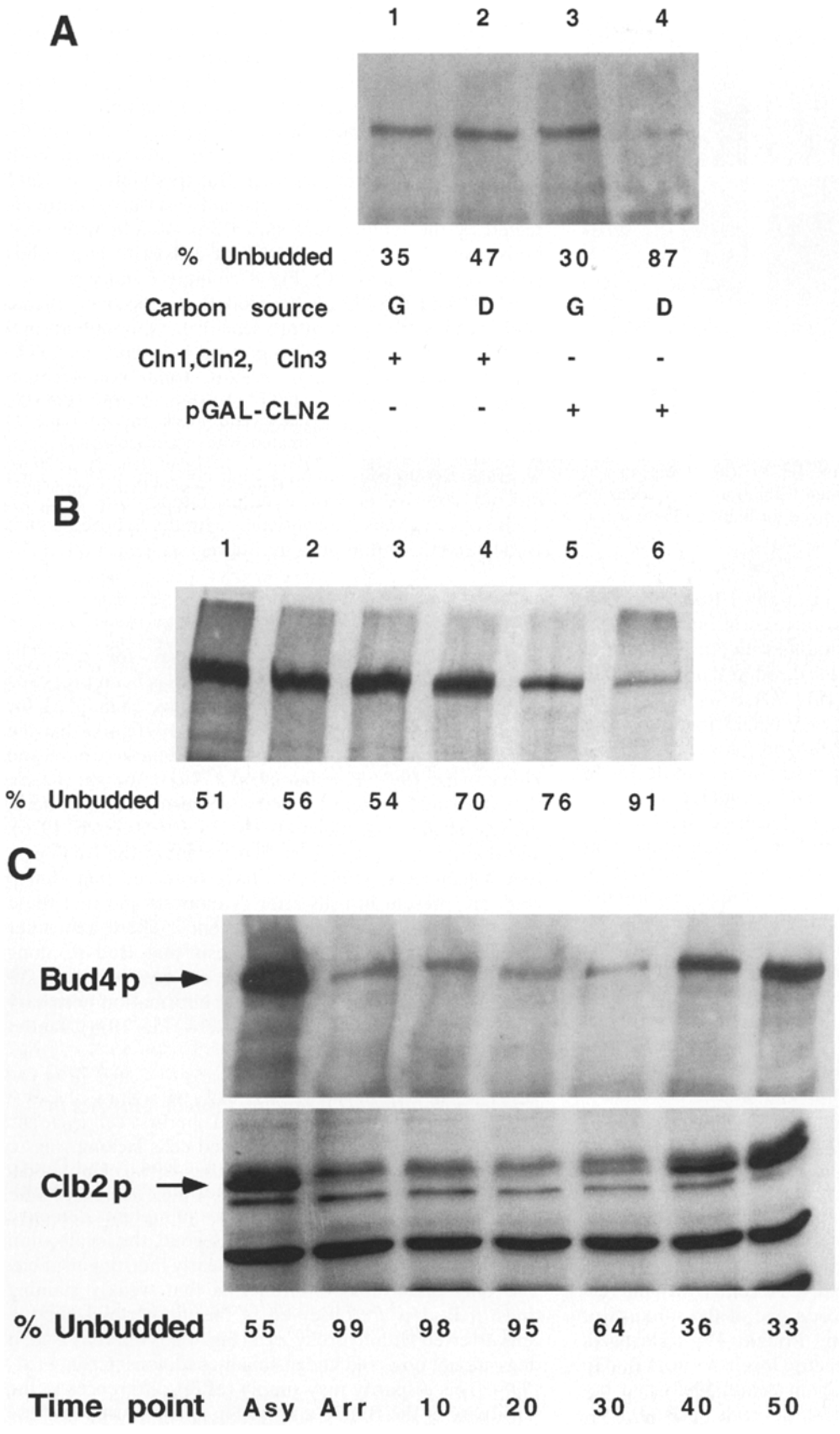

Figure 5. Absence of Bud4p from cells arrested in G1. (*A*) JO369 cells (**a** *CLN*) (lanes *1* and *2*) or ASY80 (α *Δcln1 Δcln2 Δcln3 pGAL::CLN2*) (lanes *3* and *4*) were grown to early log phase in YEP-galactose medium (lanes *1* and *3*). An aliquot of each strain was shifted to YEP-glucose medium (lanes *2* and *4*) to deplete ASY80 of Cln2p. Protein extracts were prepared from samples and subjected to analysis of Bud4p by immunoblotting. (*B*) An overnight culture of JO31-1A (**a** *BUD*) was prepared in YEPD at 30°C. Cells were diluted 50-fold into fresh medium and allowed to grow for 3 h. Samples were taken at OD_{600} of 0.19 (lane *1*), 0.34 (lane *2*), 0.95 (lane *3*), 2.6 (lane *4*), 3.5 (lane *5*), or 7.6 (lane *6*). Percentage of unbudded cells is reported below the figure. Protein extracts were prepared from samples and subjected to analysis of Bud4p by immunoblotting. Equal amounts of protein were loaded in each lane. (*C*) SY292 (**a** *BUD4*) was grown to early log phase (asynchronous culture, Asy) (lane *1*), treated with 10 μg/ml α-factor for 95 min (arrested culture, Arr) (lane *2*), and resuspended in warm, α-factor–free YEPD. Aliquots were removed every 10 min for 50 min (lanes *3–7*). Percent unbudded cells is reported below the figure. Protein extracts were prepared from samples and subjected to analysis of Bud4p by immunoblotting. Equal amounts of protein were loaded in each lane.

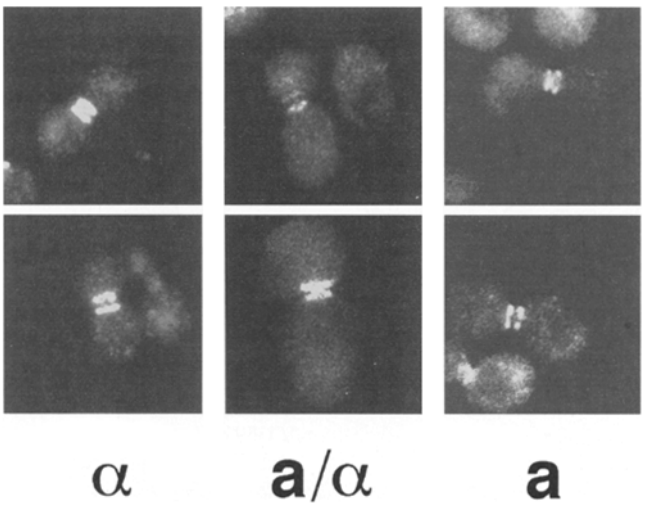

Figure 6. Localization of Bud4p in different cell types. Cells of strain IH2390 (α), IH2397 (**a**/α) and IH2393 (**a**) were grown to early log phase in YEPD and treated with 10 μg/ml nocodazole for 130 min at 25°C. Samples were fixed for immunofluorescence and stained with Bud4p antibodies.

We determined whether localization of Bud4p was dependent upon other proteins with roles in bud-site selection by examining Bud4p in mutants with altered bud-site selection patterns. Bud4p was localized at the mother/bud neck in *bud1* and *axl1* mutants (Fig. 7 *A*, rows *b* and *f*) and in *bud2-1*, *bud2::LEU2*, and *bud5::URA3* mutants (data not shown). No difference in distribution or intensity of staining was observed in comparison with Bud$^+$ cells. In contrast, the Bud4p found in *bud3-1*, *bud3::URA3*, and *bud4-1* mutants was less efficiently localized than in wild-type cells (Fig. 7 *A*, rows *c*, *d*, and *e*). Though Bud4p was visible at the mother/bud neck in the *bud3-1*, *bud3::URA3*, and *bud4-1* mutants, the staining was much less intense than in wild-type cells. As observed in wild-type cells, approximately half of all budded cells exhibited staining. Bud4p was not observed in unbudded *bud3-1* or *bud4-1* mutant cells. Absence of efficient Bud4p staining in *bud3-1* and *bud4-1* mutants was not due to reduced levels of Bud4p in those cells (Fig. 7 *B*). Bud4p was present at normal levels in extracts from all bud-site selection mutants analyzed. The Bud4p found in *bud4-1* strains exhibited a more rapid mobility in SDS-PAGE, consistent with a nonsense mutation near the 3′ end of the *BUD4* ORF or an altered posttranslational modification. The SDS-PAGE mobility of the Bud4p found in bud-site selection mutants *bud1-1*, *bud2-1*, *bud3-1*, *bud5::URA3*, and *axl1::URA3* was indistinguishable from that of Bud4p in wild-type cells (Fig. 7 *B*).

CDC12 is essential for normal yeast cell growth and cytokinesis and is thought to encode one of the subunits of the neck filaments (Haarer and Pringle, 1987; Hartwell, 1971; Longtine et al., 1996). Because localization of Bud3p requires functional *CDC12* (Chant et al., 1995) and because efficient assembly of Bud4p depends on *BUD3*, we examined the localization of Bud4p in *cdc12-6* mutants shifted to the nonpermissive temperature (37°C). Neck filaments are no longer visible in *cdc12-6* mutants shifted to the nonpermissive temperature for 5 min (Ford and Pringle, 1991; Kim et al., 1991; Chant et al., 1995; Longtine et al., 1996). Whereas localization of Bud4p appeared normal in *cdc12* mutants grown at the permissive temperature (72% of cells with large buds stained, $n = 100$) (Fig. 8, column *a*), none of the 100 cells examined exhibited Bud4p staining after a 10-min shift to 37°C (Fig. 8, column *b*). Cells stained efficiently with control antibodies at both temperatures (data not shown). Bud4p staining in *cdc12* strains bearing *CDC12* on a plasmid was only slightly affected by the temperature shift (89% of cells with large buds stained at 25°C, and 68% of cells with large buds stained at 37°C, $n = 100$) (Fig. 8, columns *c* and *d*).

BUD4 and *CDC12* also exhibited genetic interactions. *cdc12* strains are temperature sensitive, exhibiting normal growth at 25°C but failing to grow at both 30°C and 37°C (Fig. 9) (Hartwell, 1971). *cdc12-6* strains containing a *CDC12* plasmid grew well at all temperatures (Fig. 9). *BUD4* on a low copy plasmid (pSS18) partially restored growth to *cdc12-6* strains at 30°C but not at 37°C (Fig. 9) whereas *BUD4* present on a high copy plasmid (pSS17) did not improve growth at either temperature (Fig. 9). These observations are consistent with the hypothesis that Bud4p and the septin proteins interact with each other.

Discussion

The *BUD3* and *BUD4* genes are necessary for yeast cells to exhibit the axial budding pattern. It has been proposed that the Bud3 and Bud4 proteins recognize a landmark for axial budding (Chant and Herskowitz, 1991) and that the neck filaments may constitute this landmark (Chant and Herskowitz, 1991; Flescher et al., 1993). We show here that the Bud4 protein localizes to the mother/bud neck, the site of the neck filaments (Byers and Goetsch, 1976), and that its localization is similar to that of the Bud3 protein (Chant et al., 1995). We have observed that Bud4p rings are present in cells after cytokinesis and that these rings disappear before bud emergence. These and other observations support the hypothesis that Bud4p, along with Bud3p, participates in a cycle of protein–protein interactions that provides the spatial information necessary to propagate the axial budding pattern (Fig. 10) (Chant et al., 1995).

Bud4p, a Putative GTP-binding Protein, May Act in Conjunction with Bud3p

Several lines of evidence suggest that Bud3p and Bud4p act as a functional unit, perhaps forming a heteromultimeric complex. First, the phenotypes of mutants defective in *BUD3* and *BUD4* are identical. Second, the localization patterns of Bud3p and Bud4p are nearly indistinguishable. The only discernible difference is that weakly staining rings of Bud4p are observed at the mother/bud neck in cells arrested with hydroxyurea (Fig. 4 *B*), whereas Bud3p rings are not observed under similar conditions (Chant et al., 1995). This disparity may simply reflect differences in the sensitivity of the Bud3p and Bud4p antisera used in these analyses. Third, localization of both Bud3p and Bud4p depends upon the septin, *CDC12*. Finally, we have found that localization of Bud4p is strongly, although not absolutely, dependent upon *BUD3*. It is simplest to imagine

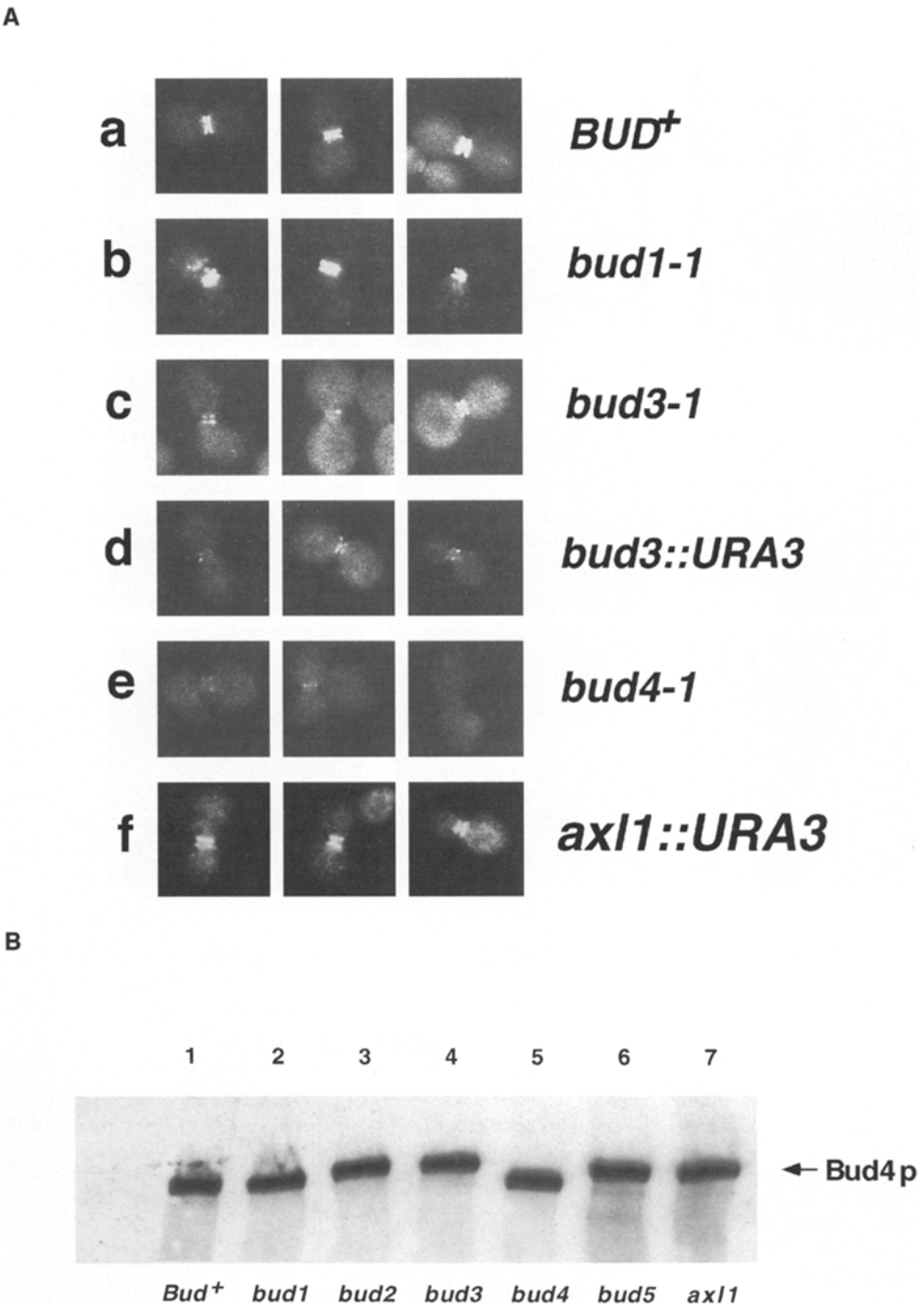

Figure 7. Requirement for *BUD3* but not *BUD1* or *AXL1* for efficient localization of Bud4p. (*A*) Cells of isogenic strains IH2393 (**a** *BUD*) (row *a*), IH2407 (**a** *bud1*) (row *b*), IH2409 (**a** *bud3*) (row *c*), MM5.1 (**a** *bud3::URA3*) (row *d*), IH2410 (**a** *bud4-1*) (row *e*), or SY401 (**a** *axl1::URA3*) (row *f*) were grown to early log phase and treated with 10 μg/ml nocodazole for 130 min. Samples were then fixed for immunofluorescence and stained with Bud4p antibodies. (*B*) Protein extracts were prepared from cells of the isogenic strains IH2393 (**a** *BUD*) (lane *1*), IH2407 (**a** *bud1*) (lane *2*); IH2408 (**a** *bud2*) (lane *3*); IH2409 (**a** *bud3*) (lane *4*); IH2410 (**a** *bud4-1*) (lane *5*); IH2424 (**a** *bud5*) (lane *6*); and SY401 (**a** *axl1::URA3*) (lane *7*) and analyzed for Bud4p by immunoblotting. Equal amounts of protein were loaded in each lane.

that Bud3p and Bud4p associate with each other to form a heteromultimeric structure.

Bud4p may be a GTP-binding protein: its carboxy terminus contains all four of the hallmark sequences found in GTPases, although it lacks consensus sequences characteristic of any particular subfamily (Fig. 2 *B*) (Bourne et al., 1991). GTP binding and hydrolysis by Bud4p could play a role at a number of different steps such as promoting localization of Bud4p to the bud site, assembly of Bud4p into ringlike structures, association of Bud4p with Bud3p or with the neck filaments, disassembly of the Bud4p rings in G1, or degradation of Bud4p. The potential GTP-binding activity of Bud4p together with its cytoskeleton-like immunofluorescence structure are reminiscent of FtsZ and the septins (for a discussion see Flescher et al., 1993). Both FtsZ and the *Drosophila* septins bind GTP and form filaments in vitro and are required for cytokinesis in vivo (de Boer et al., 1992; Field et al., 1996; Mukherjee and Lutkenhaus, 1994; Mukherjee et al., 1993; Neufeld and Rubin, 1994; RayChaudhuri and Park, 1992; Walker et al., 1975). Like Bud4p, FtsZ and the septins localize in ring structures at the site of cytokinesis (Bi and Lutkenhaus, 1991; Ford and Pringle, 1991; Haarer and Pringle, 1987; Kim et al., 1991; Neufeld and Rubin, 1994).

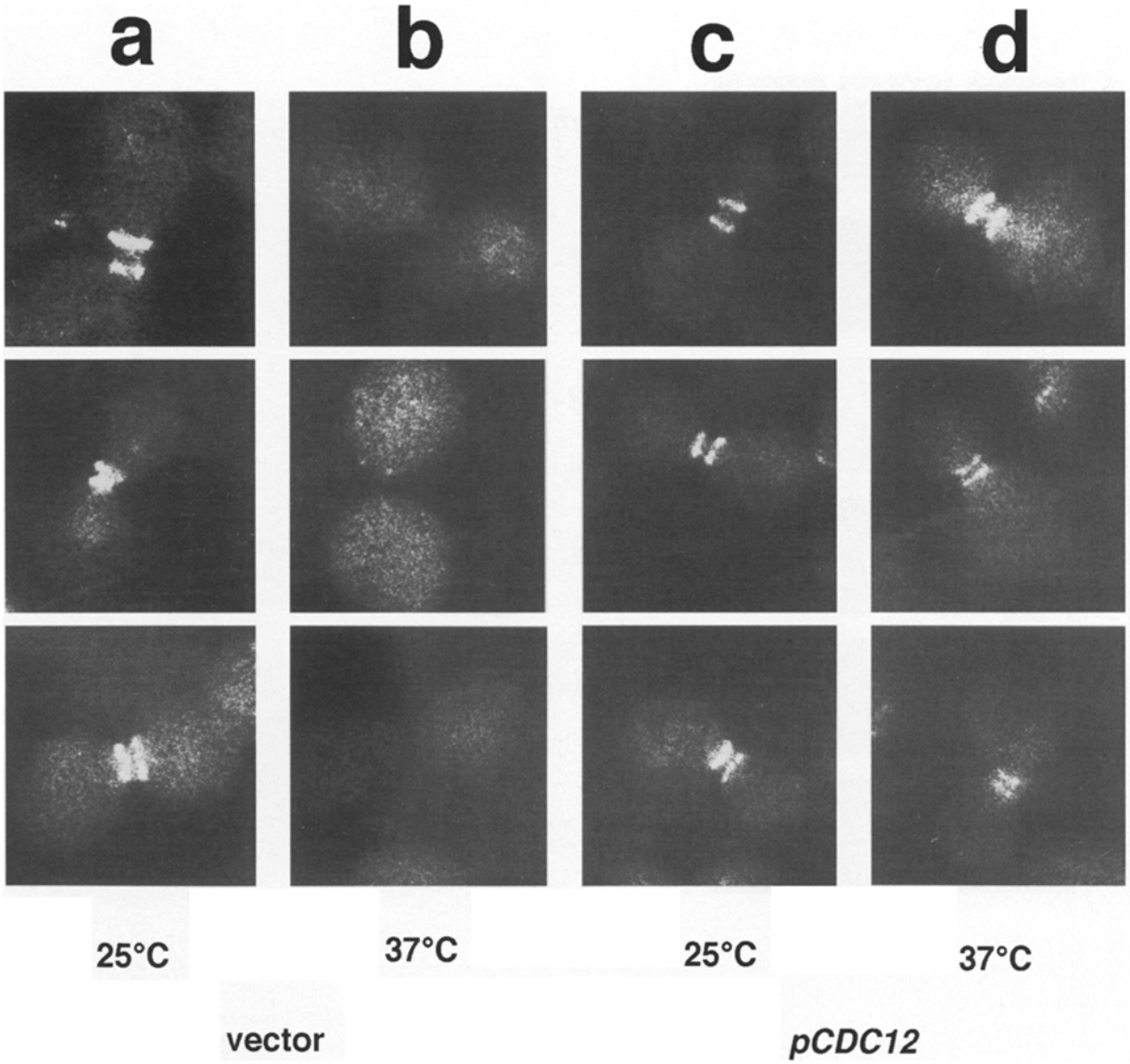

Figure 8. *CDC12* is required to maintain Bud4p at the mother/bud neck. Cells of strain SY283 (α *cdc12-6*) containing YCp50 (columns *a* and *b*) or YEp24*CDC12* (columns *c* and *d*) were grown to early log phase at 25°C in SD medium lacking uracil and then treated with 10 μg/ml nocodazole for 3 h. An aliquot was removed and fixed (25°C; columns *a* and *c*). The rest of the cultures were shifted to 37°C for 10 min and then fixed (37°C; columns *b* and *d*). Samples were processed for immunofluorescence and stained with Bud4p antibodies.

Bud4p Appears to Play a Role in a Cycle of Protein Localization

The study of Bud3p led to the proposal that Bud3p and the neck filaments determine each other's localization (Chant et al., 1995). Our findings on the localization of Bud4p are consistent with the hypothesis that Bud4p and the neck filaments likewise determine each other's localization (Fig. 10). Using synchronized cell cultures, we have shown that Bud4p rings are present after cytokinesis in early G1, where they would be in a position to determine the location of the neck filaments. Bud3p rings are also inferred to be present after cytokinesis based on comparison of Bud3p and actin staining (Chant et al., 1995). We have observed that the rings of Bud4p disappear later in G1 and are absent from cells with small buds, suggesting they are absent from cells in S phase. The Bud4p rings appear in cells with medium and large-sized buds. Analysis of Bud4p rings and protein levels in cells arrested at specific points in the cell cycle corroborated these observations. Cells arrested at START contained low levels of Bud4p, whereas cells arrested in mitosis with nocodazole contained high levels of Bud4p. Cells treated with hydroxyurea contained lower but clearly measurable levels of Bud4p, as observed for other proteins whose synthesis peaks in mitosis (for example see Sorger and Murray, 1992).

The persistence of the Bud3p and Bud4p ring structures after the neck filaments disappear at cytokinesis provides the cell with a spatial memory. Based upon electron microscopic studies (Byers and Goetsch, 1976), the neck filaments are present at the mother/bud neck from bud emer-

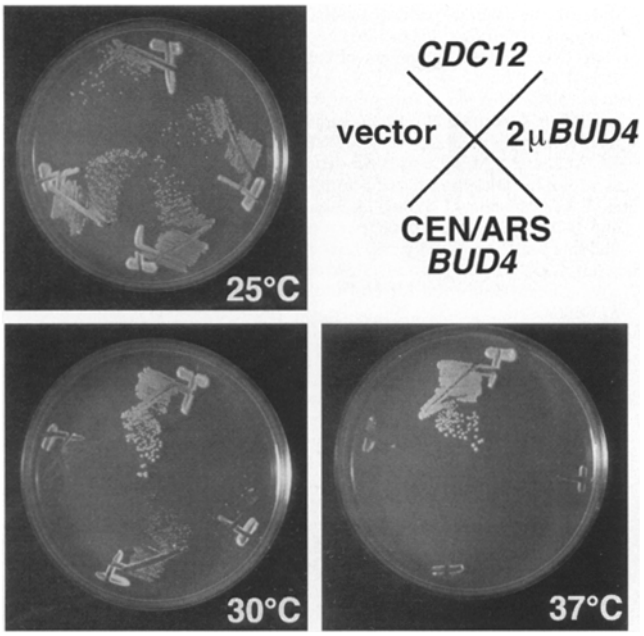

Figure 9. *BUD4* can partially suppress growth defects associated with *cdc12-6*. (*B*) SY283 (α *cdc12-6 his4 ura3*) cells transformed with pSS17 (2μ*BUD4*), pSS18 (CEN/ARS/*BUD4*), YCp50, or YEp24*CDC12* were streaked on synthetic medium lacking uracil and incubated at 25°C, 30°C, or 37°C for 3 d.

gence until cytokinesis. The septin, Cdc3p, thought to be a subunit of the neck filaments (Kim et al., 1991), arrives at the mother/bud neck shortly before bud emergence and persists until shortly after cytokinesis (Kim et al., 1991). Bud3p and Bud4p rings are present from mitosis until early G1 (Chant et al., 1995, this study). Therefore, the mother/bud neck region is marked by either Bud3p and Bud4p or the neck filaments for the entire cell cycle.

Our observation that the Bud4p rings disappear by START, before bud emergence, indicates that Bud4p (and Bud3p) function in G1 before START or perhaps even before cytokinesis. How Bud3p and Bud4p direct positioning of the new bud site is not clear at present, but they might do so by interacting with a variety of binding partners such as the neck filament proteins themselves or with proteins such as Spa2p, calmodulin, Cdc42p, Smy1p, or Myo1p, which are also localized to the nascent bud site (Brockerhoff and Davis, 1992; Lillie and Brown, 1994; Snyder et al., 1991; Ziman et al., 1993). Bud3p and Bud4p may also interact with the bud-site selection proteins Bud1p, Bud2p, and Bud5p, which are proposed to localize Cdc42p and other proteins necessary for establishing the bud site (Park et al., 1993).

Bud4p Does Not Contribute to Cell Type Differences in Budding Pattern

Because **a**/α diploids exhibit bipolar budding (as do *bud3* and *bud4* mutants), expression of *BUD3* or *BUD4* was proposed to be inhibited by **a**1-α2, a transcriptional repressor present only in **a**/α diploids (Herskowitz, 1988; Chant and Herskowitz, 1991). Both Bud3p and Bud4p, however, are present and similarly localized in all cell types (Chant et al., 1995, this study). No obvious differences in posttranslational modification of Bud4p are evident in the various cell types. The cell type differences in bud-site selection, therefore, cannot be accounted for by the presence or localization of Bud3p or Bud4p. The *AXL1* gene, also required for axial budding, is repressed in **a**/α diploids (Fujita et al., 1994). None of the currently measurable properties of Bud4p exhibit an *AXL1* dependence. In particular, Bud4p does not appear to be a target of the proteolytic activity of Axl1p as no obvious difference in molecular weight was observed for Bud4p in cells containing *AXL1* (**a** and α cells) compared to cells lacking *AXL1* (*axl1* null cells and **a**/α cells). Recent studies suggest that the proteolytic activity of Axl1p is not necessary for axial budding, although it is required for **a**-factor maturation (Adames et al., 1995). A second possible role for Axl1p would be to facilitate the localization of Bud4p. However, localization of Bud4p is indistinguishable in *AXL1* and *axl1* null mutants and in all cell types. The role of Axl1p remains to be determined.

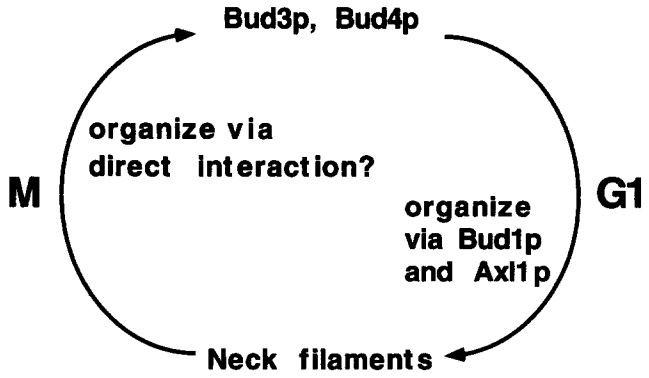

Figure 10. A cycle of protein interactions may promote axial budding. The neck filament proteins may directly bind Bud3p and Bud4p during mitosis. Bud3p and Bud4p subsequently direct the assembly of the neck filaments through the actions of Bud1p, Bud2p, Bud5p, and Axl1p in G1. See the text for details.

Regulation of Bud4p May be Responsible for Altered Polarity of Invasive, Starving, and Mating Cells

Cells recovering from starvation exhibit bipolar rather than axial budding (Chant and Pringle, 1995; Madden and Snyder, 1992; Thompson and Wheals, 1980). Because Bud4p disappears as cells become nutrient depleted, starvation conditions essentially create a phenocopy of a *bud4* mutation which causes cells to initially bud in a bipolar manner upon refeeding. Similarly, **a** and α haploid cells residing at the bottom of a colony (where they are presumably nutrient starved) exhibit nonaxial budding patterns that are either bipolar or unipolar (Roberts and Fink, 1994). We explain this altered budding pattern also as a consequence of lack of Bud4p.

Yeast cells alter their polarity program during mating (Chenevert, 1994). To mate successfully, cells must ignore axial landmarks (Dorer et al., 1995; Valtz et al., 1995; Madden and Snyder, 1992) and instead become polarized with respect to the highest concentration of pheromone of the mating partner (Jackson and Hartwell, 1990). Cells could override axial landmarks by erasing bud-site information, by building a preferred alternate site, or both. The

absence of Bud4p from cells treated with mating pheromone may facilitate choosing a new site for polarization.

Choosing sites for cell division and for orienting intracellular polarity requires that cells have the ability to position macromolecules specifically. Further studies on Bud4p and on the process by which bud sites are selected should reveal how proteins are uniquely positioned within cells and how the position of one protein influences the assembly of asymmetric structures. Our findings and those of Chant et al. (1995) suggest that Bud3p, Bud4p, and the neck filaments direct each other's assembly. Because both yeast and *Drosophila* septins are required for cytokinesis, it is possible that analogues of Bud3p and Bud4p might exist in metazoans and play a role in organizing septins or controlling other aspects of the cleavage furrow.

We thank A. Sil, M. Mischke, D. Kellogg, C. Boone, J. Li, H. Fares, T. Stearns, K. Oegema, A. Straight, and F. Banuett for their generous gifts of strains, plasmids, and oligonucleotides; C. Guthrie and M. L. Wong for photographic assistance; J. Brush for DNA sequencing; R. K. Tabtiang for identifying the putative GTP-binding motif in Bud4p; F. Banuett for suggesting that *bud4* mutant strains might form pseudohyphae; and members of the Herskowitz Lab, the UCSF Friends of Microtubules, and A. Straight for helpful advice and comments on the manuscript. S.L. Sanders was a fellow of the Helen Hay Whitney Foundation.

This work was supported by National Institutes of Health research grant GM48052.

Received for publication 22 February 1996 and in revised form 14 May 1996.

References

Adames, N., K. Blundell, M.N. Ashby, and C. Boone. 1995. Role of yeast insulin-degrading enzyme homologs in propheromone processing and bud site selection. *Science (Wash. DC).* 270:464–467.

Ausubel, F.M., R. Brent, R.E. Kingston, D.D. Moore, J.G. Seidman, J.A. Smith, and K. Struhl. 1987. Current Protocols in Molecular Biology. Greene Publishing Associates and Wiley-Interscience pp. 3.01–3.18.7.

Bender, A., and J.R. Pringle. 1989. Multicopy suppression of the *cdc24* budding defect in yeast by *CDC42* and three newly identified genes included the *ras*-related gene *RSR1*. *Proc. Natl. Acad. Sci. USA.* 86:9976–9980.

Bi, E.F., and J. Lutkenhaus. 1991. FtsZ ring structure associated with division in *Escherichia coli*. *Nature (Lond.).* 354:161–164.

Bobak, D.A., M.S. Nightingale, J.J. Murtagh, S.R. Price, J. Moss, and M. Vaughan. 1989. Molecular cloning, characterization, and expression of human ADP-ribosylation factors: two guanine nucleotide-dependent activators of cholera toxin. *Proc. Natl. Acad. Sci. USA.* 86:6101–6105.

Bourne, H.R., D.A. Sanders, and F. McCormick. 1991. The GTPase superfamily: conserved structure and molecular mechanism. *Nature (Lond.).* 349:117–127.

Brockerhoff, S.E., and T.N. Davis. 1992. Calmodulin concentrates at regions of cell growth in *Saccharomyces cerevisiae*. *J. Cell Biol.* 118:619–629.

Byers, B., and L. Goetsch. 1976. A highly ordered ring of membrane-associated filaments in budding yeast. *J. Cell Biol.* 69:717–721.

Capon, D.J., E.Y. Chen, A.D. Levinson, P.H. Seeburg, and D.V. Goeddel. 1983. Complete nucleotide sequences of the T24 human bladder carcinoma oncogene and its normal homologue. *Nature (Lond.).* 302:33–37.

Carlson, M., and D. Botstein. 1982. Two differentially regulated mRNAs with different 5′ ends encode secreted and intracellular forms of yeast invertase. *Cell.* 28:145–154.

Chant, J., and I. Herskowitz. 1991. Genetic control of bud site selection in yeast by a set of gene products that comprise a morphogenetic pathway. *Cell.* 65: 1203–1212.

Chant, J., and J.R. Pringle. 1995. Patterns of bud-site selection in the yeast *Saccharomyces cerevisiae*. *J. Cell Biol.* 129:751–765.

Chant, J., K. Corrado, J.R. Pringle, and I. Herskowitz. 1991. Yeast *BUD5*, encoding a putative GDP-GTP exchange factor, is necessary for bud site selection and interacts with bud formation gene *BEM1*. *Cell.* 65:1213–1224.

Chant, J., M. Mischke, E. Mitchell, I. Herskowitz, and J. R. Pringle. 1995. Role of Bud3p in producing the axial budding pattern of yeast. *J. Cell Biol.* 129: 767–778.

Chenevert, J. 1994. Cell polarization directed by external cues in yeast. *Mol. Biol. Cell.* 5:1169–1175.

de Boer, P., R. Crossley, and L. Rothfield. 1992. The essential bacterial cell-division protein FtsZ is a GTPase. *Nature (Lond.).* 359:254–256.

Dorer, R., P.M. Pryciak, and L.H. Hartwell. 1995. *Saccharomyces cerevisiae* cells execute a default pathway to select a mate in the absence of pheromone gradients. *J. Cell Biol.* 131:845–861.

Drubin, D.G. 1991. Development of cell polarity in budding yeast. *Cell.* 65: 1093–1096.

Field, C.M., O. Al-Awar, J. Rosenblatt, M.L. Wong, B. Alberts, and T.J. Mitchison. 1996. A purified *Drosophila* septin complex forms filaments and exhibits GTPase activity. *J. Cell Biol.* 133:605–616.

Field, C.M., and B.M. Alberts. 1995. Anillin, a contractile ring protein that cycles from the nucleus to the cell cortex. *J. Cell Biol.* 131:165–178.

Fitch, I., C. Dahmann, U. Surana, A. Amon, K. Nasmyth, L. Goetsch, B. Byers, and B. Futcher. 1992. Characterization of four B-type cyclin genes of the budding yeast *Saccharomyces cerevisiae*. *Mol. Biol. Cell.* 3:805–818.

Flescher, E.G., K. Madden, and M. Snyder. 1993. Components required for cytokinesis are important for bud site selection in yeast. *J. Cell Biol.* 122: 373–386.

Ford, S.K., and J.R. Pringle. 1991. Cellular morphogenesis in the *Saccharomyces cerevisiae* cell cycle: localization of the *CDC11* gene product and the timing of events at the budding site. *Dev. Genet.* 12:281–292.

Fujita, A., C. Oka, Y. Arikawa, T. Katagai, A. Tonouchi, S. Kuhara, and Y. Misumi. 1994. A yeast gene necessary for bud-site selection encodes a protein similar to insulin-degrading enzymes. *Nature (Lond.).* 372:567–570.

Gallwitz, D., C. Donath, and C. Sander. 1983. A yeast gene encoding a protein homologous to the human c-*has*/*bas* proto-oncogene product. *Nature (Lond.).* 306:704–707.

Ghiara, J.B., H.E. Richardson, K. Sugimoto, M. Henze, D.J. Lew, C. Wittenberg, and S.I. Reed. 1991. A cyclin B homolog in *S. cerevisiae*: chronic activation of the Cdc28 protein kinase by cyclin prevents exit from mitosis. *Cell.* 65 (1) 163–174.

Gimeno, C.J., P.O. Ljungdahl, C.A. Styles, and G.R. Fink. 1992. Unipolar cell divisions in the yeast *S. cerevisiae* lead to filamentous growth: regulation by starvation and *RAS*. *Cell.* 68:1077–1090.

Grandin, N., and S.I. Reed. 1993. Differential function and expression of *Saccharomyces cerevisiae* B-type cyclins in mitosis and meiosis. *Mol. Cell. Biol.* 13:2113–2125.

Haarer, B.K., and J.R. Pringle. 1987. Immunofluorescence localization of the *Saccharomyces cerevisiae CDC12* gene product to the vicinity of the 10-nm filaments in the mother-bud neck. *Mol. Cell. Biol.* 7:3678–3687.

Hartwell, L.H. 1971. Genetic control of the cell division cycle in yeast. IV. Genes controlling bud emergence and cytokinesis. *Exp. Cell Res.* 69:265–276.

Hartwell, L.H., J. Culotti, and B. Reid. 1970. Genetic control of the cell-division cycle in yeast. I. Detection of mutants. *Proc. Natl. Acad. Sci. USA.* 66:352–359.

Henikoff, S. 1984. Unidirectional digestion with exonuclease III creates targeted breakpoints for DNA sequencing. *Gene (Amst.).* 28:351–359.

Herskowitz, I. 1988. Life cycle of the budding yeast *Saccharomyces cerevisiae*. *Microbiol. Rev.* 52(4):536–553.

Hicks, J.B., J.N. Strathern, and I. Herskowitz. 1977. Interconversion of yeast mating types. III. Action of the homothallism (*HO*) gene in cells homozygous for the mating type locus. *Genetics.* 85:395–405.

Jackson, C.L., and L.H. Hartwell. 1990. Courtship in *S. cerevisiae*: both cell types choose mating partners by responding to the strongest pheromone signal. *Cell.* 63:1039–1051.

Jacobs, C.W., A.E.M. Adams, P.F. Szaniszlo, and J.R. Pringle. 1988. Functions of microtubules in the *Saccharomyces cerevisiae* cell cycle. *J. Cell Biol.* 107: 1409–1426.

Kellogg, D.R., A. Kikuchi, T. Fujii-Nakata, C.W. Turck, and A.W. Murray. 1995. Members of the NAP/SET family of proteins interact specifically with B-type cyclins. *J. Cell Biol.* 130:661–673.

Kim, H.B., B.K. Haarer, and J.R. Pringle. 1991. Cellular morphogenesis in the *Saccharomyces cerevisiae* cell cycle: localization of the *CDC3* gene product and the timing of events at the budding site. *J. Cell Biol.* 112:535–544.

Kron, S.J., C.A. Styles, and G.R. Fink. 1994. Symmetric cell division in pseudohyphae of the yeast *Saccharomyces cerevisiae*. *Mol. Biol. Cell.* 5:1003–1022.

Kuo, M.H., and E. Grayhack. 1994. A library of yeast genomic MCM1 binding sites contains genes involved in cell cycle control, cell wall and membrane structure, and metabolism. *Mol. Cell. Biol.* 14:348–359.

Laursen, R.A., J.J. L'Italien, S. Nagarkatti, and D.L. Miller. 1981. The amino acid sequence of elongation factor Tu of *Escherichia coli*. The complete sequence. *J. Biol. Chem.* 256:8102–8109.

Lillie, S.H., and S.S. Brown. 1994. Immunofluorescence localization of the unconventional myosin, Myo2p, and the putative kinesin-related protein, Smy1p, to the same regions of polarized growth in *Saccharomyces cerevisiae*. *J. Cell Biol.* 125:825–842.

Longtine, M.S., D.J. DeMarini, M.L. Valencik, O.S. Al-Awar, H. Fares, C. De Virgilio, and J.R. Pringle. 1996. The septins: roles in cytokinesis and other processes. *Curr. Opin. Cell Biol.* 8:106–119.

Lydall, D., G. Ammerer, and K. Nasmyth. 1991. A new role for MCM1 in yeast: cell cycle regulation of *SWI5* transcription. *Genes Dev.* 5:2405–2419.

Madaule, P., R. Axel, and A.M. Myers. 1987. Characterization of two members of the *rho* gene family from the yeast *Saccharomyces cerevisiae*. *Proc. Natl. Acad. Sci. USA.* 84:779–783.

Madden, K., and M. Snyder. 1992. Specification of sites for polarized growth in *Saccharomyces cerevisiae* and the influence of external factors on site selection. *Mol. Biol. Cell.* 3:1025–1035.

Maher, M., F. Cong, D. Kindelberger, K. Nasmyth, and S. Dalton. 1995. Cell cycle-regulated transcription of the *CLB2* gene is dependent on Mcm1 and a

ternary complex factor. *Mol. Cell. Biol.* 15:3129–3137.
Markwell, M.A.K., S.M. Haas, L.L. Bieber, and N.N. Tolbert. 1978. A modification of the Lowry procedure to simplify protein determination in membrane and lipoprotein samples. *Anal. Biochem.* 87:206–210.
Mukherjee, A., and J. Lutkenhaus. 1994. Guanine nucleotide-dependent assembly of FtsZ into filaments. *J. Bacteriol.* 176:2754–2758.
Mukherjee, A., K. Dai, and J. Lutkenhaus. 1993. *Escherichia coli* cell division protein FtsZ is a guanine nucleotide binding protein. *Proc. Natl. Acad. Sci. USA.* 90:1053–1057.
Nasmyth, K. 1983. Molecular analysis of a cell lineage. *Nature (Lond.).* 302: 670–676.
Nasmyth, K. 1993. Control of the yeast cell cycle by the Cdc28 protein kinase. *Curr. Opin. Cell Biol.* 5:166–179.
Neufeld, T.P., and G.M. Rubin. 1994. The Drosophila *peanut* gene is required for cytokinesis and encodes a protein similar to yeast putative bud neck filament proteins. *Cell.* 77:371–379.
Novick, P., and D. Botstein. 1985. Phenotypic analysis of temperature-sensitive yeast actin mutants. *Cell.* 40:405–416.
Park, H.-O., J. Chant, and I. Herskowitz. 1993. *BUD2* encodes a GTPase-activating protein for Bud1/Rsr1 necessary for proper bud-site selection in yeast. *Nature (Lond.).* 365:269–274.
Pringle, J.R. 1991. Staining of bud scars and other cell wall chitin with calcofluor. *Methods Enzymol.* 194:732–735.
Pringle, J.R., A.E.M. Adams, D.G. Drubin, and B.K. Haarer. 1991. Immunofluorescence methods for yeast. *Methods Enzymol.* 194:565–602.
RayChaudhuri, D., and J.T. Park. 1992. *Escherichia coli* cell-division gene *ftsZ* encodes a novel GTP-binding protein. *Nature (Lond.).* 359:251–254.
Rhyu, M.S., and J.A. Knoblich. 1995. Spindle orientation and asymmetric cell fate. *Cell.* 82:523–526.
Richardson, H.E., C. Wittenberg, F. Cross, and S.I. Reed. 1989. An essential G1 function for cyclin-like proteins in yeast. *Cell.* 59:1127–1133.
Richardson, H., D.J. Lew, M. Henze, K. Sugimoto, and S.I. Reed. 1992. Cyclin-B homologs in *Saccharomyces cerevisiae* function in S phase and in G2. *Genes Dev.* 6: 2021–2034.
Roberts, R.L., and G.R. Fink. 1994. Elements of a single MAP kinase cascade in *Saccharomyces cerevisiae* mediate two developmental programs in the same cell type: mating and invasive growth. *Genes Dev.* 8:2974–2985.
Robishaw, J.D., D.W. Russell, B.A. Harris, M.D. Smigel, and A.G. Gilman. 1986. Deduced primary structure of the alpha subunit of the GTP-binding stimulatory protein of adenylate cyclase. *Proc. Natl. Acad. Sci. USA.* 83: 1251–1255.
Rose, M.D., F. Winston, and P. Hieter. 1990. Methods in Yeast Genetics: A Laboratory Course. Cold Spring Harbor Laboratory Press.
Rothstein, R.J. 1983. One-step gene disruption in yeast. *Methods Enzymol.* 101: 202–211.
Sambrook, J., E.F. Fritsch, and T. Maniatis. 1989. Molecular Cloning: A Laboratory Manual. Cold Spring Harbor Laboratory Press. Cold Spring Harbor, NY. pp. 1.53–1.101, 5.3–5.86.
Sanger, F.S., S. Nicklen, and A.R. Coulson. 1977. DNA sequencing with chain-terminating inhibitors. *Proc. Natl. Acad. Sci. USA.* 75:5463–5467.
Sikorski, R.S., and P. Hieter. 1989. A system of shuttle vectors and yeast host strains designed for efficient manipulation of DNA in *Saccharomyces cerevisiae. Genetics.* 122:19–27.
Slater, M.L. 1973. Effect of reversible inhibition of deoxyribonucleic acid synthesis on the yeast cell cycle. *J. Bacteriol.* 113:263–270.
Snyder, M., S. Gehrung, and B.D. Page. 1991. Studies concerning the temporal and genetic control of cell polarity in *Saccharomyces cerevisiae. J. Cell Biol.* 114:515–532.
Sorger, P.K., and A.W. Murray. 1992. S-phase feedback control in budding yeast independent of tyrosine phosphorylation of $p34^{cdc28}$. *Nature (Lond.).* 355:365–368.
Surana, U., H. Robitsch., C. Price, T. Schuster, I. Fitch, A.B. Futcher, and K. Nasmyth. 1991. The role of *CDC28* and cyclins during mitosis in the budding yeast *S. cerevisiae. Cell.* 65:145–161.
Thompson, P.W., and A.E. Wheals. 1980. Asymmetrical division of *Saccharomyces cerevisiae* in glucose-limited chemostat culture. *J. Gen. Micro.* 121: 401–409.
Valtz, N., M. Peter, and I. Herskowitz. 1995. *FAR1* is required for oriented polarization of yeast cells in response to mating pheromones. *J. Cell Biol.* 131: 863–873.
Walker, J.R., A. Kovarik, J.S. Allen, and R.A. Gustafson. 1975. Regulation of bacterial cell division: temperature-sensitive mutants of *Escherichia coli* that are defective in septum formation. *J. Bacteriol.* 123:693–703.
Wittenberg, C., K. Sugimoto, and S.I. Reed. 1990. G1-specific cyclins of *S. cerevisiae:* cell cycle periodicity, regulation by mating pheromone, and association with the $p34^{CDC28}$ protein kinase. *Cell.* 62:225–237.
Ziman, M., D. Preuss, J. Mulholland, J.M. O'Brien, D. Botstein, and D.I. Johnson. 1993. Subcellular localization of Cdc42p, a *Saccharomyces cerevisiae* GTP-binding protein involved in the control of cell polarity. *Mol. Biol. Cell.* 4:1307–1316.